Improving olefin purification using metal organic frameworks with open metal sites

Luna-Triguero, A.; Vicent-Luna, J. M.; Poursaeidesfahani, A.; Vlugt, T. J.H.; Sánchez-De-Armas, R.; Gómez-Álvarez, P.; Calero, S.

DOI
10.1021/acsami.8b04106

Publication date
2018

Document Version
Accepted author manuscript

Published in
ACS Applied Materials and Interfaces

Improving Olefin Purification using Metal Organic Frameworks with Open Metal Sites

A. Luna-Triguero,[a] J. M. Vicent-Luna,[a] A. Poursaeidesfahani,[b] T.J.H. Vlugt,[b] R. Sánchez-de-Armas,[a] P. Gómez-Álvarez,[a]* and S. Calero[a]*

[a] Department of Physical, Chemical and Natural Systems, Universidad Pablo de Olavide, Ctra. Utrera Km 1. ES-41013, Seville, Spain.

[b] Engineering Thermodynamics, Process & Energy Department, Faculty of Mechanical, Maritime and Materials Engineering, Delft University of Technology, Leeghwaterstraat 39, 2628CB Delft, The Netherlands.

ABSTRACT: The separation and purification of light hydrocarbons is challenging in industry. Recently, ZJNU-30 metal-organic framework has been found potential for adsorption-based separation of olefins and diolefins with four carbon atoms [H. M. Liu et al. Chem. - Eur. J. 2016, 22, 14988-14997]. Our study corroborates this finding but reveals Fe-MOF-74 as a more efficient candidate for the separation due the open metal sites. We performed adsorption-base separation, transient breakthrough curves, and density functional theory calculations. This combination of techniques provides an extensive understanding of the studied system. Using this MOF we propose a separation scheme to obtain high purity product.

INTRODUCTION

The C4 olefin separation is an industrially important task. 1-butene is used as comonomer for high density polyethylene and linear low density polyethylene resins, and butylene oxide products.[1] It is also a source for heavier olefins by the metathesis reaction. 1-butene is typically produced by stream-cracking and refinery processes,[2] but these techniques generate the four isomers of butene (1-butene, 2-cis-butene, 2-trans-butene, and isobutene) as well as 1-3-butadiene. The latter is an industrial chemical used in the production of rubbers. The separation of 1-butene from the other C4 alkenes by distillation is difficult and low energy-efficient[3] due to their similar boiling points and physical properties. The boiling points of 1-butene and isobutene are particularly close to each other, and this is the reason for which chemical separation processes such as acid catalysis are needed.[4] An alternative purification method is pressure swing adsorption (PSA), using porous adsorbents to separate gas mixtures either thermodynamically or kinetically.[5-6] Zeolites are being widely studied for the separation of 1-butene from liquid or gas-phase C4 feed streams.[4, 7-9] Zeolite RUB-41 (RRO) has been reported for separation of 1-butene from 2-butenes in liquid phase since 2-butenes are more efficiently packed inside the pores than 1-butene.[4] There are also experimental and theoretical studies using Metal-Organic Frameworks (MOFs) and Zeolitic Imidazolate Frameworks (ZIFs) for this process.[10-13] Despite the efforts, to obtain high purity 1-butene is still challenging nowadays.

Recently, MOF ZJNU-30 has been synthetized and reported for butene separation.[14] Also, MOFs with open metal sites (OMS) have been proved successful for separation of saturated and unsaturated hydrocarbons due to high interaction between OMS and unsaturated hydrocarbons by the π bond.[15-16] MOF-74 has been proposed for ethane/ethene and propane/propene separation both experimentally[17-19] and theoretically,[20-21] and Fe-MOF-74 was targeted for butene isomer separation using DFT calculations.[12] A recent review on C4 hydrocarbon separations using microporous materials[22] concludes that most studies on these separations are focused on single-component gas adsorption experiments (up to 100 kPa). However, operating pressures in industrial

processes are usually higher in order to minimize costs. With this in mind, we aimed here at gaining insights into the performance of ZJNU-30 and Fe-MOF-74 for butene efficient competitive adsorption and separation. To this end, we used molecular simulation techniques as well as density functional theory. These methods are detailed in next section. The results are comprehensively discussed below and lead to a promising adsorptive-based proposal for extracting high-purity 1-butene at ambient temperature and pressures up to 1000 kPa.

METHODS

Adsorption isotherms are calculated using Monte Carlo simulations in the Grand Canonical ensemble (GCMC), where chemical potential, volume, and temperature are fixed. The chemical potential is related to the imposed fugacity, from which the pressure is determined using the Peng–Robison equation of state.[23] We perform $2 \cdot 10^5$ production run after 10^4 cycles of initialization for pure component isotherms and $5 \cdot 10^5$ production run for multicomponent isotherms to ensure an equilibrium fluctuation around a mean value of loading of adsorbates. The heat of adsorption (Q_{st}) is calculated using Widom particle insertion method[24-25] in NVT ensemble, using $5 \cdot 10^5$ and $5 \cdot 10^4$ cycles for equilibration and production runs. All these simulations were conducted at ambient temperature using RASPA code.[26-28] The structures are modelled as rigid crystals with the framework atoms placed in the crystallographic positions. For the unsaturated hydrocarbons we used united atom models.[29] The CH_3, CH_2, and CH groups are described as single interaction centers with their own effective potentials. Adsorbates are modelled as nonpolar molecules, and the possible effects of polarizability caused by the OMS and charge transfer are taken into account in Lennard-Jones (L-J) parameters. We used standard Lorentz-Berthelot (L-B) mixing rules for guest-guest interactions and specific parameters developed in previous works[20, 30] for host-guest interactions. These latter were obtained by fitting to experimental data with starting parameters calculated from L-B mixing rules and parameters given in DREIDING[31] and UFF[32] for the framework atoms and the metal sites, respectively. Indeed, studied MOFs without OMS were defined simply using these both generic force fields. As can be seen in Figure S1 of the Supporting Information (SI), the specific set of parameters accurately reproduces the experimental adsorption isotherms of the available olefins in Cu-BTC and M-MOF-74 (M=Co, Fe, Mn, and Ni). Used force field parameters for MOF-74 are listed in Table S1. For the adsorption of these compounds in zeolites, we used the force field reported in Liu et al.[33] We provide in Figure S2 a comparison between experimental and simulated isotherms of C4 olefins and diolefins in zeolites. We also performed energy minimizations for Fe-MOF-74 filling with about 18 molecules per unit cell to obtain the preferred site of adsorption. To this aim we used Baker's[34] method in NσT ensemble.

The adsorption of butene isomers on Fe-MOF-74 has been studied within density functional theory (DFT) using the Vienna ab initio simulation package (VASP) code,[35-38] employing the generalized gradient approximation (GGA) with the Perdew-Burke-Ernzerhof exchange-correlation functional[39] and projector-augmented wave (PAW) potentials.[40-41] An effective Hubbard correction of 2 eV has been used to describe the localized Fe 3d orbitals using Dudarev's approach.[42] This value has recently shown to give structures in very good agreement with experiments for hydrocarbons adsorbed on Fe-MOF-74.[43] Valence electrons are described using a plane-wave basis set with a cutoff of 500 eV and the gamma point is used for integrations in the reciprocal space.[44] We used a cell containing 162 atoms (including 18 metal centers) and we fully relaxed the structure. The calculated parameters for the bare Fe-MOF-74 unit cell are a=26.73 Å, c=6.92 Å, α=90.0, β=90.0, γ=120.0, in good agreement with previous calculations.[45] The ionic relaxation has been performed until the Hellmann-Feynman forces were lower than 0.025 eV/Å. Van der Waals interactions were taken into account through the DFT-D2 method of Grimme.[46] To study the adsorption of butene isomers on Fe-MOF-74, one molecule has been placed in the model, starting from 10 different sensible initial geometries for each molecule. We have checked that,

both for the bare MOF and after adsorption, intrachain ferromagnetic ordering and interchain antiferromagnetic ordering are always preferred.

The efficiency of an adsorbent for a certain separation is determined by the selectivity as well as by the adsorption capacity. In this sense, we also conducted transient breakthrough simulations to assess the combined effect of both properties. In our simulations, we used the methodology described in literature[47-48] and assumed: (1) the system is isothermal; (2) there is no axial dispersion; (3) radial variations in concentration are negligible com-pared to axial variations in the bed; (4) mass transfer between the gas phase and the adsorbed phase can be described by the effective LDF-model; (5) the gas phase behaves as an ideal gas. The equilibrium loadings for components present in the mixture are computed using the Ideal Adsorption Solution Theory (IAST). The material balance for each component in the gas phase is described by Eq.1.

$$\frac{1}{RT}\frac{\partial p_i}{\partial t} = -\frac{1}{RT}\frac{\partial (up_i)}{\partial t} - \left(\frac{1-\varepsilon}{\varepsilon}\right)\rho_P k_{L,i}(q_{i,eq} - \bar{q}_{i,ads}) \qquad \text{Eq(1)}$$

The system of equations is discretized in time and space using finite difference approximations and solved step wise in time. The numerical method of lines with the implicit trapezoidal rule is used to perform integration in time.

The parameters used for breakthrough simulations are as follows: Length of packed bed, L=0.3 m; voidage of packed bed, ε=0.4; superficial gas velocity in the inlet, u=0.04 m/s; the framework density of the studied MOFs is 1126.7, 1180.5, and 879.1 kg/m^3 of for Fe-MOF-74, Co-MOF-74, and Cu-BTC, respectively.

RESULTS AND DISCUSSION

ZJNU-30 is a Zr based MOF with C3-symmetrical trigonal tricarboxylate linker. The structure has a cubic symmetry with cell parameters of 28.35 Å. This MOF was reported with octahedral and cuboctahedral cages of about 14 Å and 22 Å in diameter respectively. These two cages are interconnected throught four-membered windows to form one-dimensional channels.[14] Apart from the reported cages, our calculations on pore size distribution (PSD) revealed a third cavity of about 7 Å in diameter. Figure 1a depicts the atomic connectivity and the framework cages, and the calculated PSDs are shown in Figure 1b. As it is apparent from the average occupation density profiles depicted in Figure 1c, the small cavities that we identified are inaccessible to n-butenes, but could be useful for other applications. This finding is evidenced for the specific case of 1-3-butadiene in Figure 1c left, which shows the average occupation profile obtained by Molecular Dynamics (MD) simulations for single molecules that are artificially located in the small cages. These molecules cannot cross to the other cages. A homogeneous occupation distribution is observed however when the molecule is initially placed in the large or medium-size cages (Figure 1c right). Hence, the small cages require being blocked during Monte Carlo runs for these adsorbates. As shown in Figure 2, the simulated single-component isotherms of 1-butene, 1-3-butediene, 2-cis-butene, and 2-trans-butene in the properly blocked ZJNU-30 structure are in good agreement with experimental data reported by Liu *et al*.[14] A systematical overestimation of experimental results would occur if artificial blocks were disregarded (inset Figure 2).

Figure 3 shows the adsorption behavior of 1-3-butadiene, 2-cis-butene, 2-trans-butene, and 1-butene in Fe-MOF-74 at ambient temperature. The single-component adsorption isotherms (Fig. 3a) reveal that Fe-MOF-74

exhibits the highest affinity to the diolefin: The onset adsorption fugacity of 1-3-butadiene is about one order of magnitude lower than that for the olefins. Among them, the geometrical isomer leads to an also evident adsorption discrimination, with preferential adsorption decreasing in the trend 2-cis-butene > 2-trans-butene > 1-butene. This adsorption hierarchy is the same to that found in ZJNU-30. The highest affinity of Fe-MOF-74 to the diolefin is likewise noticeable by the results for the heat of adsorption Qst, which are provided as a function of loading from isotherms in Figure 3b. However, the Qst values corresponding to the olefins are quite close. In all cases, the heat of adsorption decreases with increasing the amount of adsorbed molecules. The error in Qst is accumulative with the loading, as shown in the error bars. Results at low coverage agree well with these obtained using the Widom test-particle method: -58.2, -51.6, -48.9, and -48.3 kJ/mol for 1-3-butadiene, 2-cis-butene, 2-trans-butene, and 1-butene, respectively.

Kim et al.[12] provided theoretical calculations indicating that 1-butene could approach the metal binding sites more closely than the other butene isomers, enabling stronger bonding and π-back-bonding interactions with MOF-74. Potential π complexation is significantly hindered sterically for 2-butenes and hence their adsorption in the MOF is mainly governed by van der Waals interactions. They observed that steric repulsion follows the trend trans>cis>isobutene>1-butene, and concluded MOF-74 to be suitable for separating 1-butene from the other isomers. Liao et al.[49] conducted experimental breakthrough curves for an equimolar mixture of butane, 1-butene, isobutene, and 1-3-butadiene in Co-MOF-74, and observed a tred in such order (of citing).They provided experimental evidence that MOF-74 exhibits higher affinity to isobutene than to 1-butene. Our DFT calculations show that 1-3-butadiene has higher interaction than 1-butene in concordance with the experimental observations. Additionally, we observed that 1-butene is more stable than 2-butenes. The obtained binding energies are listed in Table S2 in SI and compared with calculations from literature.[12] We also found discrepancies in the average distances between Fe atom and C_{sp2} but the same trend (Table S3). Despite the fact that, DFT shows higher affinity of 1-butene with the metal center, we observe sligtht differences in the heat of adsorption between the isomers. The pure adsorption isotherms (Figure 3a) show different trends too and , 2-cis-butene has preferential adsorption. This could be attributed to size effects since the kinetic diameter of 2-cis-butene (4.96 Å) is considerably larger than that of 1-3-butadiene (4.31 Å), 2-trans-butene (4.31 Å), and of 1-butene (4.46 Å). [22, 50] However, adsorption of 2-trans-butene is surprisingly favored in relation to 1-butene. This could be explained in terms of a second preferential adsorption site for 2-trans-butene, which is evident from the average ocupation profiles and energy minimizations at saturation conditions depicted in Figures 4a and 4b. The new site of adsorption is due to a combination of the size effect, the weaker interaction energy and the distance to the metal center. This adsorption site is likewise observed for 1-3-butadiene due to its similar size, but it is vanished for 1-butene and 2-cis-butene. Similarly, it was found in Cu-MOF-74 for carbon dioxide, with less affinity for the molecule than the other M-MOF-74. [51] Figure 4c shows the equilibrium distances between C_{sp2} and Fe atom of the MOF, which are listed in Table S2.

In addition to the study carried out for Fe-MOF-74, we calculated pure component adsorption isotherms of of 1-3-butadiene, 2-cis-butene, 2-trans-butene, and 1-butene in Co-MOF-74 and Cu-BTC. For the latter we also calculated the adsorption isotherm of butane and isobutene in order to compare with a recently reported paper that provides the experimental breakthrough for an equimolar mixture of 1-3-butadiene, 1-butene, butane, and isobutene.[49] The adsorption isotherms of the single components in Fe-MOF-74, Co-MOF-74 and Cu-BTC were fitted using Lagmuir-Freundlich dual-site model (Figure S3 and S4). The fitting parameters are listed in Tables S3-

S5 in the SI. We performed breakthrough calculations of the mentioned mixture for Cu-BTC and the four-component equimolar mixture of 1-3-butadiene, 2-cis-butene, 2-trans-butene, and 1-butene in Cu-BTC, Co-MOF-74, and Fe-MOF-74 at total pressure of 100 kPa. We obtained for Cu-BTC the following adsorption hierarchy: butane>1-butene>isobutene>1-3-butadiene (Figure S5). This finding is in agreement with the experimental breakthrough repoted for the same mixture.[49] The sequence of the calculated breakthrough (Figure 5 and S5-S6) on the three structures is 1-butene> 2-trans-butene> 2-cis-butene > 1-3-butadiene which matches with the above-reported competitive adsorption of the mixture.

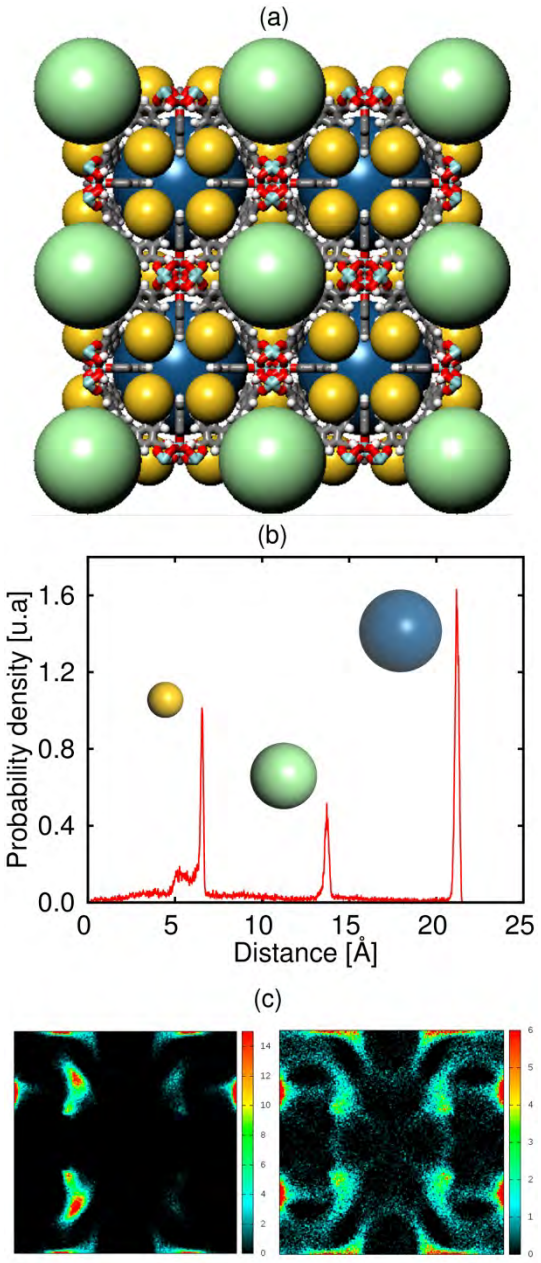

Figure 1. (a) Schematic representation of the atomic connectivity of ZJNU-30. Carbon atoms in grey, oxygen atoms in red, hydrogen atoms in white, and zirconium atoms in turquois. The spheres represent the pore cages. (b) Pore size distribution of ZJNU-30. (c) Average occupation profiles for ZJNU-30 from MD simulations using one molecule of 1-3-butadiene (left: initial position in small cages, right: initial position in large or medium cages).

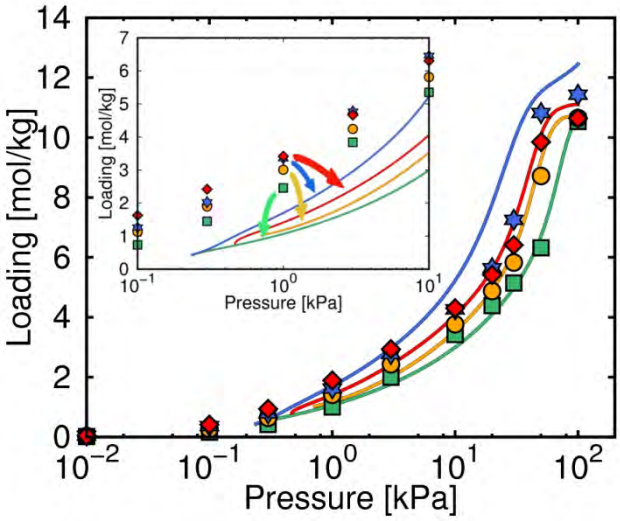

Figure 2. Calculated (symbols) and experimental isotherms (lines)[14] of 2-cis-butene (blue), 2-trans-butene (red), 1-butene (yellow), and 1-3-butadiene (green) in ZJNU-30 at 298 K. Inset figure shows the calculated values (symbols) if appropriate pore blocks are disregarded.

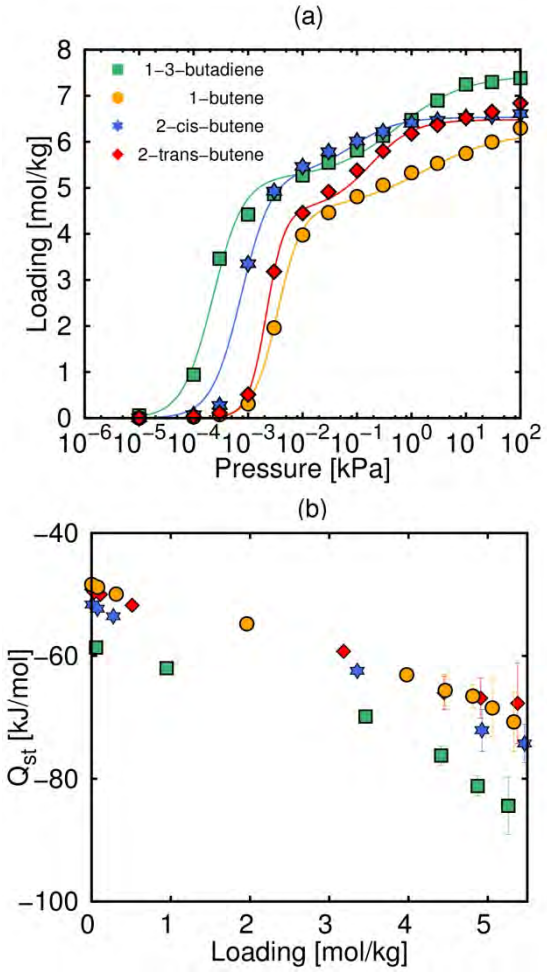

Figure 3. (a) Pure adsorption isotherms (symbols) and isotherm fits (lines) and (b) heat of adsorption as a function of loading of 1-3-butadiene, 1-butene, 2-cis-butene, and 2-trans-butene in Fe-MOF-74 at 298 K.

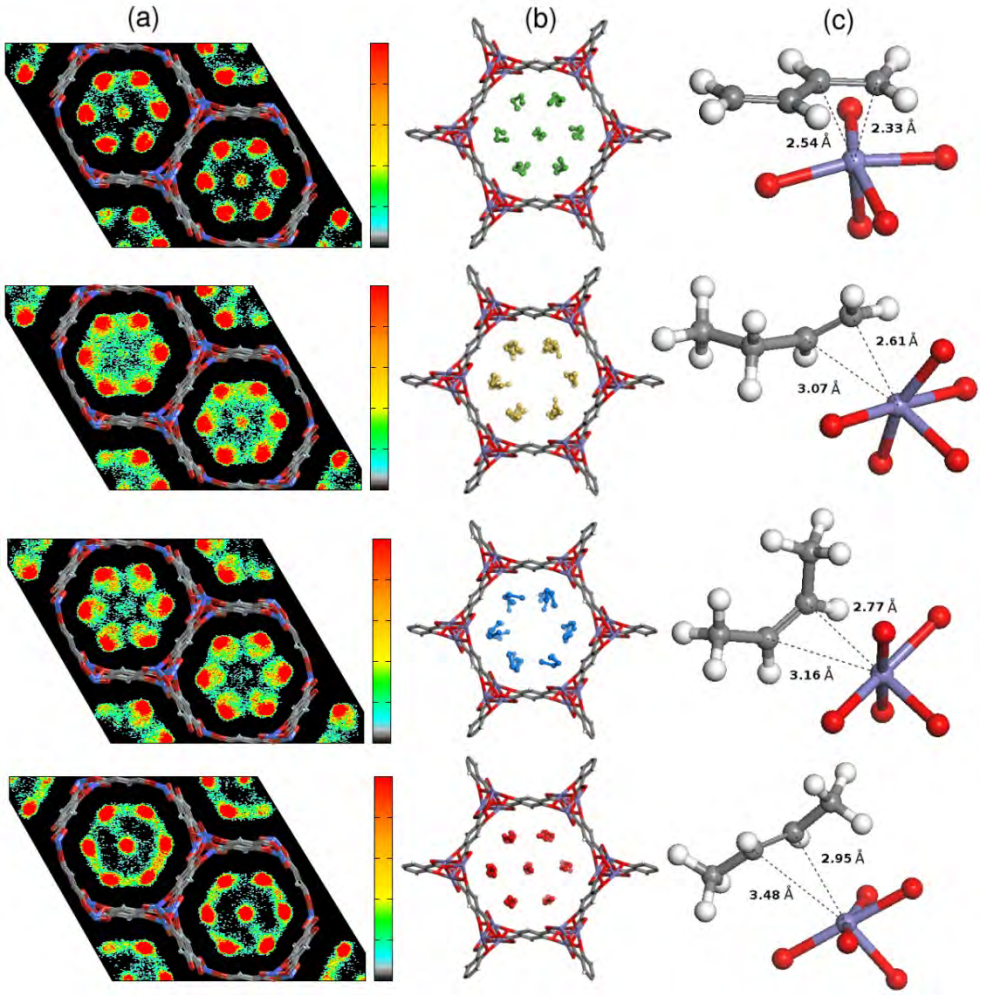

Figure 4. (a) Average occupation profiles, (b) and equilibrium positions from classical minimizations at saturation conditions, and (c) equilibrium distances between C sp2 and metal center of structure from DFT calculations. From top to bottom: 1-3-butadiene, 1-butene, 2-cis-butene, and 2-trans-butene in Fe-MOF-74.

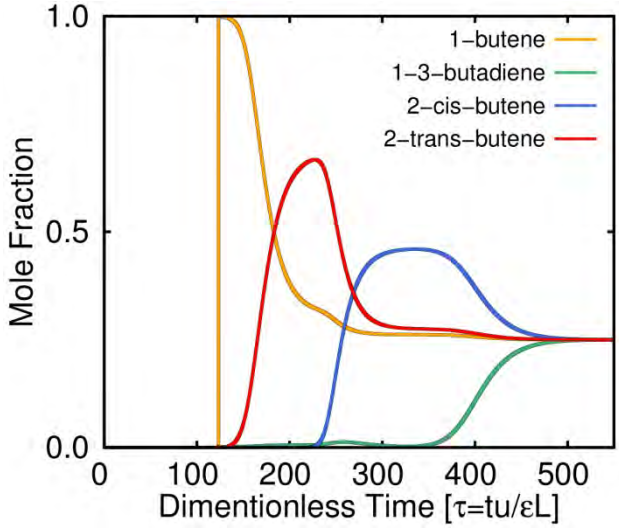

Figure 5. Transient breakthrough simulations for the separation of an equimolar multicomponent mixture of 1-3-butadiene, 1-butene, 2-cis-buetene, and 2-trans-butene in Fe-MOF-74 at 298 K.

The adsorption selectivity $S_{AB} = (x_A/y_A)/(x_B/y_B)$ gauges if a material exhibits selective adsorption for a component A over B. This value is calculated straightforward from the molar fractions in the adsorbed phase (x_A, x_B) and the molar fractions in the bulk phase (y_A, y_B). Figure 6 depicts adsorption selectivities of ZJNU-30 and Fe-MOF-74 calculated from the equimolar four-component mixture of 1-butene, butadiene, 2-cis-butene, and 2-trans-butene at 298 K. The adsorption loadings from the multicomponent mixture in Fe-MOF-74 were obtained by conducting GCMC simulations using a specifically developed force field.[20] For ZJNU-30, we used Ideal Adsorbed Solution Theory (IAST)[52-53] and pure component experimental isotherms provided by Liu *et al.*[14] We found adsorption selectivity to be independent of pressure in ZJNU-30 and to reach the highest values at low pressure (from 0.1 Pa to 10 Pa) in Fe-MOF-74. This is ascribed to the differences in the onset pressures of adsorption of the compounds in this MOF. In Figure 6 we plot the adsorption selectivity at 10 kPa. We choose this value because it is a practical operational condition and, at this pressure the loadings are already large enough to obtain reliable adsorption selectivity. ZJNU-30 and Fe-MOF-74 favor the adsorption for different butene isomers. The adsorption selectivity in Fe-MOF-74 is always in favor of the diolefin, whereas ZJNU-30 preferentially adsorbs the cis- and trans- isomers. In both structures the cis-/trans- selectivity is similar, and the less adsorbed component is 1-butane for Fe-MOF-74 and the diolefin for ZJNU-30.

Another interesting finding is that Fe-MOF-74 exhibits larger selectivity values than ZJNU-30. The selectivity of 1-3 butadiene over 1-butene is 50 times larger in Fe-MOF-74 than in ZJNU-30 because of the higher interaction of the double bond and the metallic center of the structure with OMS.

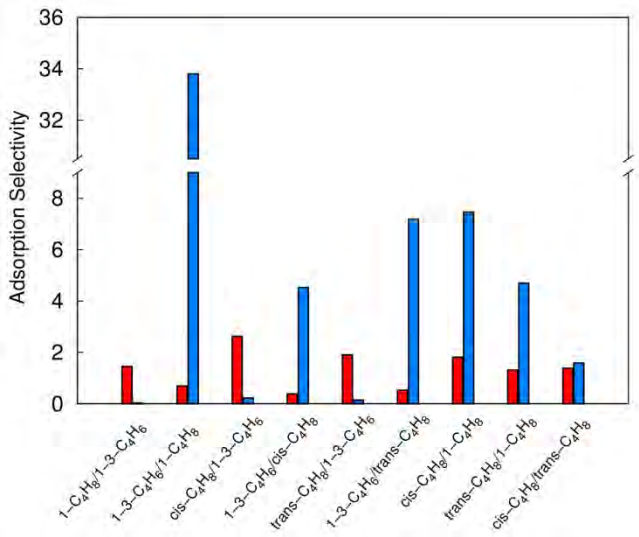

Figure 6. Adsorption selectivity for 2-cis-butene/1-3-butadiene, 1-3-butadiene/2-cis-butene, 2-trans-butene/1-3-butadiene, 1-3-butadiene/2-trans-butene, 2-cis-butene/1-butene, 2-trans-butene/1-butene, and 2-cis-butene/2-trans-butene calculated from the a adsorption isotherms of equimolar quaternary mixtures in ZJNU-30 and Fe-MOF-74 at 298 K and 10 kPa.

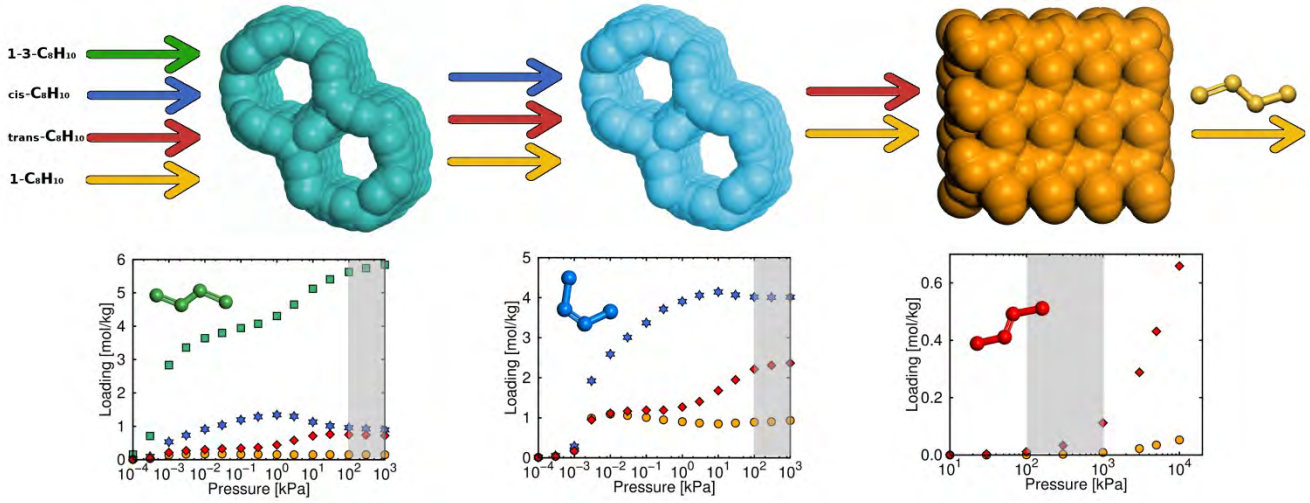

Figure 7. Proposed adsorptive-based separation process of 1-butene from C4 alkene mixture. Multicomponent adsorption isotherms in Fe-MOF-74 (a, b) and RRO zeolite (c) at 298 K. 2-cis-butene (blue), 2-trans-butene (red), 1-butene (yellow), and 1-3-butadie (green).

Overall, we found Fe-MOF-74 unquestionably more selective than ZJNU-30 for butene separation. Hence, we can use this MOF to obtain high purity 1-butene from C4 feed streams at ambient temperature and operational pressures from 100kPa to 1000kPa (Figure 7). First, Fe-MOF-74 can be used to separate the diolefin 1-3 butadiene from the other components of the equimolar quaternary mixture (left plot). This MOF is also suitable for the separation of 2-cis-butene from the remaining ternary mixture of 2-cis butene (24%), 2-trans butene (30%) and 1-butene (46%) (center plot). Finally, the separation of 1-butene from 2-trans-butene can be satisfactorily addressed using RRO zeolite. The competitive adsorption of the 1-butene (72%) / 2-trans butene (28%) binary mixture in this zeolite results in the exclusion of 1-butene yielding a 94% of purity product for the operating conditions (right plot).

CONCLUSIONS

In summary, MOFs with OMs are able to sepatate diolefines from 1-butene, 2-trans-butene, and 2-cis-butene due the higher affinity with the metal center of the structure. In particular, GCMC simulations and DFT calculations evidence this higher interaction for the diolefin with the Fe atom of MOF-74. The separation between 2-cis butene from the remaining butene isomers is due to the steric effects. We found a new site of adsorption showed by 2-trans-butene which explains its higher saturation in pure adsorption isotherm than for 1-butene. Basis on this findings we propose an adsorptive-base separation process which explote the ability of MOF-74 to separate the diolefine and 2-cis-butene from the studied mixture. We propose the separation of remaining compounds (1-butene and 2-trans-butene) using zeolite RRO. The hierarchy showed by adsorptive separation is supported by breakthrough curves.

AUTHOR INFORMATION

Corresponding Author

pgomalv1@upo.es

scalero@upo.es

Notes

The authors declare no competing financial interests.

ACKNOWLEDGMENT

This work was supported by the Spanish Ministerio de Economía y Competitividad (CTQ2016-80206-P). The authors also gratefully acknowledge the financial support from Shell Global Solutions B.V., and the Netherlands Research Council for Chemical Sciences (NWO/CW) through a VICI grant (Thijs J. H. Vlugt).

REFERENCES

1. Alsadoun, A. W., Dimerization of Ethylene to Butene-1 Catalyzed by Ti(or')4-Alr3. *Applied Catalysis a-General* **1993**, *105*, 1-40.
2. Aljarallah, A. M.; Anabtawi, J. A.; Siddiqui, M. A. B.; Aitani, A. M.; Alsadoun, A. W., Ethylene Dimerization and Oligomerization to Butene-1 and Linear Alpha-Olefins - a Review of Catalytic-Systems and Processes. *Catal. Today* **1992**, *14*, R9-&.
3. Herm, Z. R.; Bloch, E. D.; Long, J. R., Hydrocarbon Separations in Metal-Organic Frameworks. *Chem. Mater.* **2014**, *26*, 323-338.
4. Tijsebaert, B.; Varszegi, C.; Gies, H.; Xiao, F. S.; Bao, X. H.; Tatsumi, T.; Muller, U.; De Vos, D., Liquid Phase Separation of 1-Butene from 2-Butenes on All-Silica Zeolite Rub-41. *Chem. Commun.* **2008**, 2480-2482.
5. Sircar, S., Basic Research Needs for Design of Adsorptive Gas Separation Processes. *Ind. Eng. Chem. Res.* **2006**, *45*, 5435-5448.
6. Yang, R., Gas Separation by Adsorption Processesimperial College Press. London: 1997.
7. Jousse, F.; Leherte, L.; Vercauteren, D. P., Analysis of Md Trajectories as a Jump Diffusion Process: Butene Isomers in Zeolite Types Ton and Mel. *J. Phys. Chem. B* **1997**, *101*, 4717-4732.
8. Jousse, F.; Auerbach, S. M.; Vercauteren, D. P., Capturing the Concentration Dependence of Trans-2-Butene Diffusion in Silicalite-2 Zeolite with a Jump Diffusion Model. *J. Phys. Chem. B* **1998**, *102*, 6507-6514.
9. Zhu, W.; Kapteijn, F.; Moulijn, J. A.; Jansen, J. C., Selective Adsorption of Unsaturated Linear C-4 Molecules on the All-Silica Dd3r. *Phys. Chem. Chem. Phys.* **2000**, *2*, 1773-1779.
10. Alaerts, L.; Maes, M.; van der Veen, M. A.; Jacobs, P. A.; De Vos, D. E., Metal–Organic Frameworks as High-Potential Adsorbents for Liquid-Phase Separations of Olefins, Alkylnaphthalenes and Dichlorobenzenes. *Phys. Chem. Chem. Phys.* **2009**, *11*, 2903-2911.
11. van den Bergh, J.; Gücüyener, C.; Pidko, E. A.; Hensen, E. J.; Gascon, J.; Kapteijn, F., Understanding the Anomalous Alkane Selectivity of Zif-7 in the Separation of Light Alkane/Alkene Mixtures. *Chemistry–A European Journal* **2011**, *17*, 8832-8840.
12. Kim, H.; Jung, Y., Can Metal-Organic Framework Separate 1-Butene from Butene Isomers? *J. Phys. Chem. Lett.* **2014**, *5*, 440-446.
13. Kishida, K.; Okumura, Y.; Watanabe, Y.; Mukoyoshi, M.; Bracco, S.; Comotti, A.; Sozzani, P.; Horike, S.; Kitagawa, S., Recognition of 1,3-Butadiene by a Porous Coordination Polymer. *Angew. Chem., Int. Ed.* **2016**, *55*, 13784-13788.
14. Liu, H. M.; He, Y. B.; Jiao, J. J.; Bai, D. J.; Chen, L.; Krishna, R.; Chen, B. L., A Porous Zirconium-Based Metal-Organic Framework with the Potential for the Separation of Butene Isomers. *Chem. - Eur. J.* **2016**, *22*, 14988-14997.
15. Bae, Y.-S.; Lee, C. Y.; Kim, K. C.; Farha, O. K.; Nickias, P.; Hupp, J. T.; Nguyen, S. T.; Snurr, R. Q., High Propene/Propane Selectivity in Isostructural Metal–Organic Frameworks with High Densities of Open Metal Sites. *Angew. Chem.* **2012**, *51*, 1857-1860.

16. Bao, Z.; Alnemrat, S.; Yu, L.; Vasiliev, I.; Ren, Q.; Lu, X.; Deng, S., Adsorption of Ethane, Ethylene, Propane, and Propylene on a Magnesium-Based Metal–Organic Framework. *Langmuir* **2011**, *27*, 13554-13562.
17. Geier, S. J.; Mason, J. A.; Bloch, E. D.; Queen, W. L.; Hudson, M. R.; Brown, C. M.; Long, J. R., Selective Adsorption of Ethylene over Ethane and Propylene over Propane in the Metal-Organic Frameworks M-2(Dobdc) (M = Mg, Mn, Fe, Co, Ni, Zn). *Chem. Sci.* **2013**, *4*, 2054-2061.
18. Bloch, E. D.; Queen, W. L.; Krishna, R.; Zadrozny, J. M.; Brown, C. M.; Long, J. R., Hydrocarbon Separations in a Metal-Organic Framework with Open Iron(Ii) Coordination Sites. *Science* **2012**, *335*, 1606-1610.
19. He, Y.; Krishna, R.; Chen, B., Metal-Organic Frameworks with Potential for Energy-Efficient Adsorptive Separation of Light Hydrocarbons. *Energy Environ. Sci.* **2012**, *5*, 9107-9120.
20. Luna-Triguero, A.; Vicent-Luna, J. M.; Becker, T. M.; Vlugt, T. J. H.; Dubbeldam, D.; Gómez-Álvarez, P.; Calero, S., Effective Model for Olefin/Paraffin Separation Using (Co,Fe, Mn, Ni)-Mof-74. *ChemistrySelect* **2017**.
21. Verma, P.; Xu, X. F.; Truhlar, D. G., Adsorption on Fe-Mof-74 for C1-C3 Hydrocarbon Separation. *J. Phys. Chem. C* **2013**, *117*, 12648-12660.
22. Gehre, M.; Guo, Z.; Rothenberg, G.; Tanase, S., Sustainable Separations of C4-Hydrocarbons by Using Microporous Materials. *Chemsuschem* **2017**, *10*, 3947-3963.
23. Peng, D.-Y.; Robinson, D. B., A New Two-Constant Equation of State. *Ind. Eng. Chem. Fundam.* **1976**, *15*, 59-64.
24. Widom, B., Some Topics in the Theory of Fluids. *J. Chem. Phys.* **1963**, *39*, 2808-2812.
25. Poursaeidesfahani, A.; Torres-Knoop, A.; Rigutto, M.; Nair, N.; Dubbeldam, D.; Vlugt, T. J., Computation of the Heat and Entropy of Adsorption in Proximity of Inflection Points. *J. Phys. Chem. C* **2016**, *120*, 1727-1738.
26. Dubbeldam, D.; Torres-Knoop, A.; Walton, K. S., On the Inner Workings of Monte Carlo Codes. *Mol. Simul.* **2013**, *39*, 1253-1292.
27. Dubbeldam, D.; Calero, S.; Ellis, D. E.; Snurr, R. Q., Raspa: Molecular Simulation Software for Adsorption and Diffusion in Flexible Nanoporous Materials. *Mol. Simul.* **2015**, *42*, 81-101.
28. Dubbeldam, D.; Snurr, R. Q., Recent Developments in the Molecular Modeling of Diffusion in Nanoporous Materials. *Mol. Simul.* **2007**, *33*, 305-325.
29. Wick, C. D.; Martin, M. G.; Siepmann, J. I., Transferable Potentials for Phase Equilibria. 4. United-Atom Description of Linear and Branched Alkenes and Alkylbenzenes. *The Journal of Physical Chemistry B* **2000**, *104*, 8008-8016.
30. Luna-Triguero, A.; Vicent-Luna, J. M.; Gómez-Álvarez, P.; Calero, S., Olefin/Paraffin Separation in Open Metal Site Cu-Btc Metal–Organic Framework. *J. Phys. Chem. C* **2017**, *121*, 3126-3132.
31. Mayo, S. L.; Olafson, B. D.; Goddard, W. A., Dreiding - a Generic Force-Field for Molecular Simulations. *J. Phys. Chem* **1990**, *94*, 8897-8909.
32. Rappe, A. K.; Casewit, C. J.; Colwell, K. S.; Goddard, W. A.; Skiff, W. M., Uff, a Full Periodic-Table Force-Field for Molecular Mechanics and Molecular-Dynamics Simulations. *J. Am. Chem. Soc.* **1992**, *114*, 10024-10035.
33. Liu, B.; Smit, B.; Rey, F.; Valencia, S.; Calero, S., A New United Atom Force Field for Adsorption of Alkenes in Zeolites. *J. Phys. Chem. C* **2008**, *112*, 2492-2498.
34. Baker, J., An Algorithm for the Location of Transition States. *J. Comput. Chem.* **1986**, *7*, 385-395.
35. Kresse, G.; Hafner, J., Ab Initio Molecular Dynamics for Liquid Metals. *Physical Review B* **1993**, *47*, 558.
36. Kresse, G.; Hafner, J., Ab Initio Molecular-Dynamics Simulation of the Liquid-Metal-Amorphous Semiconductor Transition in Germanium. *Physical Review B* **1994**, *49*, 14251-14269.
37. Kresse, G.; Furthmuller, J., Efficiency of Ab-Initio Total Energy Calculations for Metals and Semiconductors Using a Plane-Wave Basis Set. *Computational Materials Science* **1996**, *6*, 15-50.
38. Kresse, G.; Furthmuller, J., Efficient Iterative Schemes for Ab Initio Total-Energy Calculations Using a Plane-Wave Basis Set. *Physical Review B* **1996**, *54*, 11169-11186.
39. Perdew, J. P.; Burke, K.; Ernzerhof, M., Generalized Gradient Approximation Made Simple. *Physical Review Letters* **1996**, *77*, 3865-3868.
40. Blochl, P. E., Projector Augmented-Wave Method. *Physical Review B* **1994**, *50*, 17953-17979.
41. Kresse, G.; Joubert, D., From Ultrasoft Pseudopotentials to the Projector Augmented-Wave Method. *Physical Review B* **1999**, *59*, 1758-1775.

42. Dudarev, S. L.; Botton, G. A.; Savrasov, S. Y.; Humphreys, C. J.; Sutton, A. P., Electron-Energy-Loss Spectra and the Structural Stability of Nickel Oxide: An Lsda+U Study. *Physical Review B* **1998**, *57*, 1505-1509.
43. Verma, P.; Maurice, R.; Truhlar, D. G., Adsorbate-Induced Changes in Magnetic Interactions in Fe-2(Dobdc) with Adsorbed Hydrocarbon Molecules. *Journal of Physical Chemistry C* **2016**, *120*, 9933-9948.
44. Monkhorst, H. J.; Pack, J. D., Special Points for Brillouin-Zone Integrations. *Physical Review B* **1976**, *13*, 5188-5192.
45. Lee, K.; Howe, J. D.; Lin, L. C.; Smit, B.; Neaton, J. B., Small-Molecule Adsorption in Open-Site Metal-Organic Frameworks: A Systematic Density Functional Theory Study for Rational Design. *Chem. Mat.* **2015**, *27*, 668-678.
46. Grimme, S., Semiempirical Gga-Type Density Functional Constructed with a Long-Range Dispersion Correction. *Journal of Computational Chemistry* **2006**, *27*, 1787-1799.
47. Krishna, R., The Maxwell–Stefan Description of Mixture Diffusion in Nanoporous Crystalline Materials. *Microporous Mesoporous Mater.* **2014**, *185*, 30-50.
48. Krishna, R.; Long, J. R., Screening Metal–Organic Frameworks by Analysis of Transient Breakthrough of Gas Mixtures in a Fixed Bed Adsorber. *J. Phys. Chem. C* **2011**, *115*, 12941-12950.
49. Liao, P.-Q.; Huang, N.-Y.; Zhang, W.-X.; Zhang, J.-P.; Chen, X.-M., Controlling Guest Conformation for Efficient Purification of Butadiene. *Science* **2017**, *356*, 1193-1196.
50. Gucuyener, C.; van den Bergh, J.; Joaristi, A. M.; Magusin, P. C. M. M.; Hensen, E. J. M.; Gascon, J.; Kapteijn, F., Facile Synthesis of the Dd3r Zeolite: Performance in the Adsorptive Separation of Buta-1,3-Diene and but-2-Ene Isomers. *J. Mater. Chem.* **2011**, *21*, 18386-18397.
51. Queen, W. L.; Hudson, M. R.; Bloch, E. D.; Mason, J. A.; Gonzalez, M. I.; Lee, J. S.; Gygi, D.; Howe, J. D.; Lee, K.; Darwish, T. A., Comprehensive Study of Carbon Dioxide Adsorption in the Metal–Organic Frameworks M 2 (Dobdc)(M= Mg, Mn, Fe, Co, Ni, Cu, Zn). *Chem. Sci.* **2014**, *5*, 4569-4581.
52. Myers, A.; Prausnitz, J. M., Thermodynamics of Mixed-Gas Adsorption. *AIChE J.* **1965**, *11*, 121-127.
53. Balestra, S. R. G.; Bueno-Perez, R.; Calero, S., Gaiast. Zenodo, 2016.

Insert Table of Contents artwork here